NATIONAL ADVISORY COMMITTEE FOR AERONAUTICS

TECHNICAL NOTE 3893

THEORY AND DESIGN OF A PNEUMATIC TEMPERATURE PROBE AND EXPERIMENTAL RESULTS OBTAINED IN A HIGH-TEMPERATURE GAS STREAM

By Frederick S. Simmons and George E. Glawe

Lewis Flight Propulsion Laboratory
Cleveland, Ohio

Washington
January 1957

TABLE OF CONTENTS

NATIONAL ADVISORY COMMITTEE FOR AERONAUTICS

TECHNICAL NOTE 3893

THEORY AND DESIGN OF A PNEUMATIC TEMPERATURE PROBE AND EXPERIMENTAL RESULTS OBTAINED IN A HIGH-TEMPERATURE GAS STREAM

By Frederick S. Simmons and George E. Glawe

SUMMARY

The basic theory of pneumatic temperature probes and deviations from this basic theory in practical application are presented. Design requirements and operating considerations are discussed. Temperatures between 1600° and 4000° R were measured with an experimental probe in hydrocarbon combustion exhaust gases and compared with those measured by thermocouples and a line-reversal pyrometer. Reasonable agreement among the instruments was obtained.

INTRODUCTION

An accurate temperature measurement of a gas stream becomes increasingly difficult with increasing temperature, and most of the better known methods have some shortcomings. For example, immersion instruments such as thermocouples or resistance thermometers that are capable of withstanding high temperatures require large corrections of the indications to account for heat-transfer and recovery effects. Optical techniques, such as sodium-line reversal, usually measure some mean temperature along the optical path and require the presence of chemicals in the gas stream.

A method which appears to offer several advantages is the use of a pneumatic temperature probe. This instrument consists essentially of two restrictions through which a sample of the hot gas is successively passed and between which the gas is cooled. From continuity of mass, the stream temperature is a function of the pressure measured at each restriction, the temperature at the downstream restriction, and the areas and discharge coefficients of the restrictions. Thus, a thermodynamic measurement of gas temperature can be obtained beyond the range of most commonly used thermocouple materials.

Publications (through 1951) on pneumatic-probe methods of measuring gas temperature are listed in reference 1, and later work is described in references 2 and 3. This report reviews some of the considerations

entering into pneumatic-probe design and compares a pneumatic probe with thermocouple pyrometers and a line-reversal pyrometer. The pneumatic probe herein described used a nozzle for the upstream restriction and a venturi tube for the downstream restriction, with sonic flow through both restrictions. Measurements were made in the temperature range from 1600° to 4000° R, at subsonic stream Mach numbers, and at static pressures of the order of 1 atmosphere. This work is part of the research program in high-temperature measurements being conducted at the NACA Lewis laboratory.

THEORY

Basic Equations

A schematic diagram of the pneumatic probe with pressure and temperature notation is shown in figure 1. (Symbols are defined in appendix A.)

The basic equation for mass-flow rate, which assumes that a perfect gas is expanded isentropically and one-dimensionally in an orifice, is given by

$$w = \frac{PA}{\sqrt{T}}\sqrt{\frac{2}{R}}\sqrt{\frac{\gamma}{\gamma - 1}\left[\left(\frac{p}{P}\right)^{\frac{2}{\gamma}} - \left(\frac{p}{P}\right)^{\frac{\gamma+1}{\gamma}}\right]} \tag{1}$$

Defining a discharge coefficient C as the ratio of the actual mass-flow rate to the ideal mass-flow rate and equating the actual mass-flow rates of the two restrictions in series yield, for constant R:

$$C_2 \frac{P_0}{\sqrt{T_0}} A_2 \sqrt{\frac{\gamma_{0,2}}{\gamma_{0,2} - 1}\left[\left(\frac{p_2}{P_0}\right)^{\frac{2}{\gamma_{0,2}}} - \left(\frac{p_2}{P_0}\right)^{\frac{\gamma_{0,2}+1}{\gamma_{0,2}}}\right]}$$

$$= C_4 \frac{P_3}{\sqrt{T_3}} A_4 \sqrt{\frac{\gamma_{3,4}}{\gamma_{3,4} - 1}\left[\left(\frac{p_4}{P_3}\right)^{\frac{2}{\gamma_{3,4}}} - \left(\frac{p_4}{P_3}\right)^{\frac{\gamma_{3,4}+1}{\gamma_{3,4}}}\right]} \tag{2}$$

Solving for the temperature ahead of the front nozzle gives

$$T_0 = T_3\left(\frac{C_2}{C_4}\frac{A_2}{A_4}\frac{P_0}{P_3}\frac{F_1}{F_3}\right)^2 \tag{3a}$$

where

$$F_1 \equiv \sqrt{\frac{\gamma_{0,2}}{\gamma_{0,2} - 1}\left[\left(\frac{p_2}{P_0}\right)^{\frac{2}{\gamma_{0,2}}} - \left(\frac{p_2}{P_0}\right)^{\frac{\gamma_{0,2}+1}{\gamma_{0,2}}}\right]}$$

$$F_3 \equiv \sqrt{\frac{\gamma_{3,4}}{\gamma_{3,4} - 1}\left[\left(\frac{p_4}{P_3}\right)^{\frac{2}{\gamma_{3,4}}} - \left(\frac{p_4}{P_3}\right)^{\frac{\gamma_{3,4}+1}{\gamma_{3,4}}}\right]}$$

Application of equation (3a) to a pneumatic temperature probe in general involves the measurement of the pressures P_0, p_2, P_3, and p_4 and the temperature T_3; calculation of the quantities F_1 and F_3 from the measured pressures with knowledge of the effective specific-heat ratios $\gamma_{0,2}$ and $\gamma_{3,4}$; and knowledge of the ratios C_2/C_4 and A_2/A_4.

For the special case where the flow through both restrictions is sonic, it can be shown that

$$T_0 = T_3\left(\frac{C_2}{C_4}\frac{A_2}{A_4}\right)^2\left(\frac{P_0}{P_3}\right)^2\left[\frac{F_s(\gamma_{0,2})}{F_s(\gamma_{3,4})}\right]^2 \tag{3b}$$

where

$$F_s(\gamma) = \frac{\sqrt{\gamma/2}}{\left(\frac{\gamma+1}{2}\right)^{\frac{\gamma+1}{2(\gamma-1)}}}$$

If it is assumed that C_2A_2/C_4A_4 is a constant and $\gamma_{0,2} = \gamma_{3,4}$, equation (3b) reduces to

$$T_0 = \text{Constant} \times T_3\left(\frac{P_0}{P_3}\right)^2 \tag{3c}$$

Effects of Heat Transfer on Nozzle Discharge Coefficient

The quantity $(C_2A_2/C_4A_4)^2$ in equation (3b) is usually considered as a constant. In practice, there are variations in this quantity

resulting from changes in the physical areas of the nozzles and variation in the discharge coefficients with Reynolds number and heat transfer between the gas and the nozzle surfaces. It is difficult to determine $(A_2/A_4)^2$ accurately by direct physical measurement of the nozzle throats, since this quantity is proportional to the fourth power of the diameters. However, from equation (3a) it can be seen that

$$\left(\frac{C_2A_2}{C_4A_4}\right)^2_{T_0=T_3} = \left(\frac{P_3}{P_0}\frac{F_3}{F_1}\right)^2_{T_0=T_3}$$

Therefore, the quantity $(C_2A_2/C_4A_4)^2$ can be obtained by a calibration, that is, operation of the probe at room temperature where $T_0 = T_3$. The factor $(C_2/C_4)^2$ can then be computed from known relations between discharge coefficients and Reynolds numbers and separated from the term $(C_2A_2/C_4A_4)^2$. This development thus yields an effective area factor $(A_2/A_4)^2$ which in application would be altered only by thermal expansion or erosion and particle deposition. The effect of thermal expansion for a hot run can be calculated with knowledge of nozzle temperatures or can be reduced to a negligible quantity by proper cooling of the restrictions. The effects of erosion or particle deposition can be accounted for by periodic calibration at room temperature.

The quantity $(C_2/C_4)^2$ to be applied to the solution of T_0 for a hot run can be treated by using the expression suggested in reference 4, which shows that the discharge coefficient of a flow nozzle, when the fluid is a gas and there is heat transfer between gas and nozzle, is

$$C = 1 - \frac{7}{\sqrt{Re_{D_{th}}}}\sqrt{\frac{l}{D_{th}} + \frac{1}{4}\frac{l'}{D_{th}}}\, f\left(\frac{t}{t_n}\right) \qquad (4)$$

where t/t_n is the ratio of gas to nozzle-wall temperature, l the length of straight throat section, l' the axial length of the rounded approach section, D_{th} the nozzle throat diameter, and

$$f\left(\frac{t}{t_n}\right) \equiv \frac{1 - \frac{\ln\left(\frac{t}{t_n}\right)}{\ln 2}}{2 - \frac{t}{t_n}}$$

The calculation of C_2 involves the Reynolds number of the upstream nozzle; this Reynolds number is a function of the temperature of the gas which is being measured. An iterative calculation would, therefore, be

necessary, but an adequate value of T_0 for this Reynolds number can be obtained from equation (3c) using the value of $(C_2A_2/C_4A_4)^2$ obtained in a cold calibration. The computations are facilitated by the use of figure 2, which shows the Reynolds number for critical flow through a 1/8-inch-diameter nozzle as a function of gas temperature and pressure, and figure 3, which is a plot of equation (4) for the nozzle used ($D = 2l = l'$).

Effective Specific-Heat Ratio

Equation (1) was derived on the assumption that the ratio of specific heats of the gas is a quantity independent of the process the gas undergoes. At room temperature this is true for real gases, but as the temperature is increased, energy absorbed by internal vibration of the molecules becomes increasingly important. Consequently, the specific heats and their ratio become functions of temperature. However, the transfer of energy into the vibrational mode does not occur with the same rapidity as that among the rotational and translational modes, the reason being that only certain types of collisions, which occur relatively infrequently, can excite a molecule in vibration. A characteristic or relaxation time for the vibrational mode of the gas may be defined and shown to be a function of the pressure, temperature, and composition of the gas. Thus, should a gas undergo a change, for instance, an expansion, in a time much shorter than the vibrational relaxation time, the process would correspond to one in which γ retains a value corresponding to the absence of any vibrational degrees of freedom. Reference 5 is concerned with this effect in flow processes involving hydrocarbon products.

Three other effects further complicate the problem of the nozzle flow processes occurring in a pneumatic probe:

(1) If the pneumatic probe is immersed in a high-velocity gas stream, a compression and an expansion, not necessarily of like duration, occur at the upstream nozzle.

(2) If the gas stream is of sufficiently high temperature that dissociation is appreciable, the cooling of the gas within the probe would involve an uncertain degree of recombination with resultant uncertainty in the specific-heat ratio and the gas constant.

(3) Most gases of interest are mixtures; a net effect would involve combinations and interactions of the preceding effects among the components.

An approximation for the case where the compression ahead of the upstream nozzle occurs in a time of the same order as the relaxation time for the hydrocarbon gases is presented in appendix B. A relation

is established wherein an effective $\gamma_{0,2}$ is related to equilibrium high-temperature γ_0, equilibrium low-temperature $\gamma_{3,4}$, and free-stream Mach number.

PROBE DESCRIPTION AND DESIGN CONSIDERATIONS

Probe Description

A photograph of the experimental probe is shown in figure 4; details of the first-nozzle assembly, which had a 1/8-inch-diameter throat, are shown in figure 5. The second nozzle was geometrically similar with the exception of a diffuser section, which in effect made it a venturi tube. Both nozzles were constructed from a chrome-copper alloy. The probe was designed for testing at gas-stream total pressures of the order of 1 atmosphere to utilize the large-capacity laboratory exhaust system (approximate pressure, 10 in. Hg abs) for pumping. A diameter ratio $D_{th,2}/D_{th,4}$ of unity was chosen to ensure sonic flow in both nozzles at the anticipated range of high-temperature operation. The thermocouple for measuring gas temperature T_3 was chromel-alumel, 0.010 inch in diameter, and had an immersion length of 50 diameters.

5040

Design Considerations

Choice of restriction shape. - The restriction configurations of the probe described were chosen because:

(1) Some preliminary experiments in exhaust gas streams containing a relatively large amount of unburned solid particles had shown that throat area and discharge coefficient were changed less by erosion and by dirt deposition in the case of flow nozzles than in the case of sharp-edged orifices.

(2) It was felt that constancy of throat area could best be maintained if the restriction were cooled and that this cooling could be effected more easily for a thin-walled nozzle than for a sharp-edged orifice.

(3) At constant Reynolds number, the discharge coefficient of the nozzle remains constant with pressure ratio in supercritical flow (ref. 6), whereas that of the sharp-edged orifice does not.

(4) Pressure loss at the downstream restriction was least for the venturi-type design; thus, severity of pumping requirements was minimized.

The disadvantages of the nozzle are:

(1) The effect of heat transfer from the gas to the cooled surface of the nozzle is greater than that for the sharp-edged orifice. This heat transfer affects the boundary-layer flow and hence the discharge coefficient.

(2) Mechanical construction of a nozzle is more difficult than that of a sharp-edged orifice.

5040

(3) For throat diameters in the range of 0.04 to 0.1 inch, the variation of discharge coefficient with Reynolds number at constant pressure ratio is greater for a nozzle than it is for a sharp-edged orifice.

The advantages itemized for the nozzle were considered to outweigh the disadvantages, since an approximate theory was available to correct for the effect of heat transfer on the discharge coefficient (ref. 4).

The size of the throat diameter chosen was based upon a compromise between pumping requirements and the advantage of a large throat area in achieving high Reynolds numbers and minimizing effects of dirt deposition.

Pumping requirements. - Pumping requirements may be estimated by using equation (3a) and assuming $C_2/C_4 = F_1/F_3 = 1$ and by choosing a convenient temperature T_3. This temperature is chosen high enough to be well above the dew point and low enough to be measured accurately.

Then equation (3a) becomes

$$\frac{P_3}{P_0} = \left(\frac{D_{th,2}}{D_{th,4}}\right)^2 \sqrt{\frac{T_3}{T_0}} \tag{5}$$

Assuming sonic flow in the first nozzle and slight pressure loss between stations 2 and 3 gives

$$\frac{P_3}{P_0} \leq \frac{P_2}{P_0} \approx \frac{1}{2} \tag{6}$$

so that the required diameter ratio is specified by the inequality

$$\frac{D_{th,2}}{D_{th,4}} \leq \sqrt{\frac{1}{2}} \sqrt[4]{\frac{T_0}{T_3}} \tag{7}$$

Assuming sonic flow in the second nozzle and 60-percent recovery of the velocity head in the diffuser, the approximate pressure ratio at the second nozzle is

$$\frac{P_4}{P_3} \approx \frac{1}{2} \tag{8}$$

Therefore,

$$\frac{P_5}{P_3} \approx 0.8 \tag{9}$$

If sonic flow exists also in the first nozzle, equations (6) and (9) yield

$$P_5 \leq 0.4\ P_0 \tag{10}$$

This inequality establishes the pumping pressure that must be maintained at the downstream end of the probe to achieve sonic flow in both nozzles at high-temperature operation. Availability of adequate pumping facilities to maintain this over-all pressure ratio would eliminate the necessity of measuring static pressures p_2 and p_4, which need be known only if sonic flow does not exist in both nozzles. From equation (7) it can be seen that when $T_0 = T_3$ the diameter ratio $D_{th,2}/D_{th,4}$ must be equal to or less than 0.7 for sonic flow to exist in both nozzles. However, for this case the pumping requirements would be more severe at high-temperature operation. For a diameter ratio of unity, subsonic flow will exist in the first nozzle for a calibration at $T_0 = T_3$, but sonic flow in both nozzles at high-temperature operation can then be attained with less severe pumping capacity.

Cooling requirements. - Conventional heat-transfer formulas are adequate for probe cooling calculations. By arbitrarily selecting some fixed dimensions and from knowledge of anticipated operating conditions, the dependent quantities such as coolant flow rate and pressure drop can be found. A detailed procedure for calculation is presented in appendix C.

Pressure and Temperature Measurements

The use of the pneumatic probe involves, in the most general case, the measurement of four pressures, one gas temperature, and two nozzle wall temperatures.

The total pressure P_0 of the gas stream may be measured by any of three approaches: A separate total-pressure probe can be used; the flow in the probe can be stopped, and the P_3 gage used to make the measurement; or a pressure tap can be provided on the face of the upstream nozzle (P_1). In this last method, however, the total pressure P_1 so

measured was not fully equal to P_0, and varied primarily with Mach number, so that a pressure calibration relating P_1/P_0 to Mach number M was required (fig. 6). The measurement of P_0 with a separate probe, whenever possible, appears to be the most advantageous method. Measurement by the P_1 tap not only has the defect previously noted, but also suffers from the fact that small tubing must be used which penalizes the response time. The method of stopping the flow in the probe has the disadvantage that a P_3 gage would have to be used which has a greater range than would be necessary for the measurement of P_3 under flow conditions. Also, the possibility of internal condensation would present the problem of time necessary to reestablish continuity of mass when the pumping is resumed.

Static pressures p_2 and p_4 need be measured only if there is any uncertainty that sonic flow exists in both nozzles. Measurements made with the p_2 and p_4 taps on the present probe confirmed that equations (7) and (10) were reasonable approximations and sonic flow existed at both restrictions.

The measurement of total pressure P_3 upstream of the second nozzle can be obtained with a wall tap if the duct area upstream of the second nozzle is sufficiently large to substantially constitute a stagnation region.

The region upstream of the second nozzle is then also a convenient location for measurement of total temperature T_3 by means of a thermocouple. This temperature should also be sufficiently low so that the radiation and conduction errors of the thermocouple are negligible.

Knowledge of the nozzle wall temperature was necessary for the computation of discharge coefficient under the condition of heat transfer (ref. 4). Experiments with some preliminary probe designs had shown that, with the cooling arrangement shown in figure 5, the nozzle wall temperature did not greatly exceed the water temperature. Hence, direct measurement of nozzle wall temperature by thermocouples was not necessary.

APPARATUS

High-Temperature Tunnel

The tests were performed in the high-temperature water-cooled tunnel described in reference 7. This facility is capable of continuous operation at temperatures from 1400° to 3700° R, Mach numbers from 0.2 to 1.0, and pressures from 1/2 to 2 atmospheres. Using oxygen, operation for short periods to a temperature of 4000° R is possible within restricted ranges of velocity and pressure. The fuel throughout these

tests was 60-octane gasolene. Total pressure was measured with a water-cooled probe upstream of the 4-inch nozzle, and static pressure by a measurement of receiver pressure.

Comparison Instruments

An aspirated chromel-alumel thermocouple probe was used for comparison from 1600° to 2500° R. Reference 8 shows data indicating this probe to be sensibly free from radiation and conduction errors in the range of conditions encountered in these tests.

Two bare-wire, butt-welded, platinum-13-percent-rhodium - platinum thermocouples with water-cooled supports were also used for comparison. One platinum thermocouple was a 0.020-inch-diameter wire with an immersion length of 50 diameters, and the other platinum thermocouple was a 0.032-inch-diameter wire with an immersion length of 28 diameters. The junctions of these thermocouples were butt-welded and then swaged to reduce the welding "bead" to wire diameter so that the configuration represented a cylinder in crossflow with uniform diameter. The sodium-line-reversal instrument was essentially a self-balancing adaptation of the standard instrument and is described in detail in reference 9.

TESTS AND RESULTS

Calibration Tests

The calibration coefficient $(C_2A_2/C_4A_4)^2$ was experimentally obtained using room-temperature air, at total pressures from 20 to 50 inches of mercury absolute, and at Mach numbers from 0 to 1.0. The value obtained was constant to within the experimental accuracy. The mean value of $(A_2/A_4)^2$ was found to be 0.842. The nozzle-throat diameters were specified as being equal, so theoretically this factor should be unity. The calibration therefore indicates that the actual nozzle diameters were approximately within 2 percent of specified diameter assuming one oversize and the other undersize. These results indicate the importance of a calibration, since an error of about 16 percent in T_0 would result from assuming $(A_2/A_4)^2$ to be unity.

High-Temperature Tests and Results

The experimental pneumatic probe was tested from 1600° to 4000° R at a stream total pressure of 1 atmosphere and at Mach numbers of the order of 0.5 in overlapping ranges of the comparison instruments previously described.

To eliminate effects of gradients in temperature and pressure, the comparison between probes was made by moving each probe, in turn, to the same location in the gas stream with tunnel conditions held constant.

For the line-reversal measurement, sodium bicarbonate powder was injected into the gas stream through a water-cooled probe upstream of the test region. This method of injection provided a local stream of sodium vapor in the test section so that a localized temperature was obtained. During injection of the compound, the other instruments were retracted to avoid particle deposition.

During the tests, the temperature ahead of the second nozzle T_3 was of the order of 700° R. The pneumatic-probe temperatures were calculated by equation (3b) with the following assumptions:

(1) The effective specific-heat ratio $\gamma_{0,2}$ can be calculated by the method presented in appendix B.

(2) The effect of heat transfer on the nozzle discharge coefficients can be calculated by equation (4) with nozzle wall temperature taken as the mean cooling-water temperature.

The radiation, conduction, and recovery corrections of the platinum thermocouple probes were calculated by using methods and values given in references 7 and 10. The maximum total correction for the 0.020-inch-diameter platinum thermocouple was 270° F, and the maximum total correction for the 0.032-inch-diameter platinum thermocouple was 360° F. The results of these comparisons are plotted in figure 7(a). At 3700° R the agreement with comparison instruments was of the order of ±2 percent.

These data for the pneumatic probe were also computed by using the calibration value of $(C_2A_2/C_4A_4)^2$ in equation (3b), in order to show the result of neglecting the heat-transfer and Reynolds number effect on the coefficient of discharge of the nozzles. The results of this computation are in figure 7(b), and they show a systematic error.

In tests made at Mach numbers from 0.3 to 1.0 at a stream total temperature of 2460° R the comparison instrument was the aspirated chromel-alumel thermocouple. The results of these tests are shown in figure 8. The squares represent temperatures calculated using $\gamma_{0,2} = \gamma_{1,2} = \gamma_{3,4}$ and show a marked dependence on stream Mach number. From this result equation (B5) was deduced. Temperatures calculated using equations (B5) and (B6) are indicated in the same figure by the circles. It is noted that the corrections bring the pneumatic-probe data to within about 1 percent of the comparison instrument. A sample calculation is given in appendix E.

The gas stream was sufficiently clean that systematic changes in the coefficient $(C_2A_2/C_4A_4)^2$ as determined by calibrations with room-temperature air before and after each series of tests were less than 1 percent. The average duration of exposure was about 1 hour.

DISCUSSION

In view of the lack of a means of accurately establishing the true gas temperature in these tests, the absolute accuracy, as such, of the pneumatic probe cannot be stated. However, the agreement among the methods, as shown in figure 7(a), is fairly satisfactory from 1600° to 3800° R.

Above 3800° R the pneumatic probe indicates considerably higher temperatures than those of the sodium-D-line-reversal instrument. A possible cause is the fact that these data were taken using oxygen in addition to air in the combustion. The pneumatic-probe temperatures were calculated using the same assumptions as for hydrocarbon-air combustion. Not only are these assumptions questionable, but at these temperatures the effects of dissociated water vapor and carbon dioxide in the products become apparent. A detailed analysis of these factors was considered to be beyond the scope of the present work. Furthermore, from the experimental procedure, it is felt that errors exist in the D-line measurements at these higher temperatures such as those due to sodium contamination (ref. 9). The experimental procedure involved the addition of oxygen to a very rich fuel-air mixture while observing the indication of a platinum thermocouple located in the cooler outer boundary of the jet. While the thermocouple indication and the pneumatic-probe temperature increased uniformly with increasing amount of oxygen, the D-line temperature showed little or no increase.

The data shown in figure 8 indicate that errors of the order of 5 percent may result from not considering the compression ahead of the upstream nozzle when the probe is immersed in a gas stream of Mach number near unity. The empirical relations represented by equations (B5) and (B6) were selected from these data, which were obtained at a fairly accurately measurable gas temperature of 2460° R.

The use of equations (4) and (B6) which take into account heat transfer and effects of flow variations, respectively, in the nozzles may be considered as corrections to the basic equation (3c) of the pneumatic probe. Because the corrections are, at most, a few percent in magnitude, the validity of equations (4) and (B6) is not clearly shown by the experimental results, particularly in the instances where the corrections tend to counteract one another, such being the case in the sample calculation. On the other hand, since the corrections are small, the use of

crude assumptions in the derivation of the equations is justified in that large errors may be present in the corrections without introducing significant errors in the temperature measurements.

Appendix D shows orders of magnitude of the various possible errors mentioned throughout the text.

CONCLUDING REMARKS

An experimental probe based on the design criteria herein reported was operated to 4000° R and compared with other types of pyrometers. Reasonable agreement among the instruments was obtained. The following recommendations based on this investigation are made:

1. Flow nozzles should be chosen in preference to thin-plate orifices.

2. Temperature ahead of the downstream nozzle should be low enough to be accurately measured, but above the dewpoint of the gas at the pressure ahead of the downstream nozzle.

3. Sonic velocity should be maintained in both nozzles when the probe is used to obtain free-stream total temperature. A nozzle diameter ratio of unity can be used to decrease pumping requirements, in which case the room-temperature calibration must accept subsonic flow in the first nozzle.

4. Free-stream total pressure should be measured with a separate total-pressure probe if possible.

Lewis Flight Propulsion Laboratory
National Advisory Committee for Aeronautics
Cleveland, Ohio, October 12, 1956

APPENDIX A

SYMBOLS

The following symbols are used in this report:

A	cross-sectional area of nozzle throat
C	discharge coefficient
c_p	specific heat of gas at constant pressure
c_w	specific heat of water
D	diameter
F	$\sqrt{\frac{\gamma}{\gamma - 1}\left[\left(\frac{p}{P}\right)^{2/\gamma} - \left(\frac{p}{P}\right)^{\frac{\gamma+1}{\gamma}}\right]}$
$F_s(\gamma)$	$\frac{\sqrt{\frac{\gamma}{2}}}{\left(\frac{\gamma + 1}{2}\right)^{\frac{\gamma+1}{2(\gamma-1)}}}$
f	function
g	acceleration due to gravity
k	thermal conductivity
L	probe length
l	length of straight section of nozzle
l^*	axial length of approach section of nozzle
M	Mach number
P	total pressure
p	static pressure
q	heat-transfer rate

5040

R	specific gas constant
Re	Reynolds number
T	total temperature
t	static temperature
W	fraction of water vapor in gas
w	ideal mass-flow rate
x	wall thickness
y	radial depth
γ	specific-heat ratio
ρ	density of gas
μ	viscosity of gas
τ	relaxation time of gas

Subscripts:

e	external
g	gas
i	internal
n	wall at nozzle throat
r	reference
s	sonic
th	throat
w	cooling water
0	free stream
1	immediately ahead of upstream nozzle
2	throat of upstream nozzle

3 ahead of downstream nozzle

4 throat of downstream nozzle

5 behind downstream nozzle

APPENDIX B

ESTIMATION OF EFFECTIVE SPECIFIC-HEAT RATIO

Effective values of the specific-heat ratio for the flow process at the upstream nozzle may be defined by the following equations which assume the velocity at station (1) to be zero and the flow to be one-dimensional:

$$\left.\begin{aligned} \frac{T_0}{t_0} &= 1 + \frac{\gamma_0 - 1}{2} M_0^2 \\ \frac{T_1}{t_0} &= 1 + \frac{\gamma_{0,1} - 1}{2} M_0^2 \\ \frac{T_1}{t_2} &= 1 + \frac{\gamma_{1,2} - 1}{2} M_2^2 \end{aligned}\right\} \tag{B1a}$$

The temperature ratio for the entire process is described by

$$\frac{T_0}{t_2} = 1 + \frac{\gamma_{0,2} - 1}{2} M_2^2 \tag{B1b}$$

where the effective specific-heat ratio of the entire process $\gamma_{0,2}$ is obtained by simultaneous solution of equations (B1)

$$\gamma_{0,2} = 1 + \frac{2}{M_2^2}\left[\frac{\left(1 + \frac{\gamma_{1,2} - 1}{2} M_2^2\right)\left(1 + \frac{\gamma_0 - 1}{2} M_0^2\right)}{\left(1 + \frac{\gamma_{0,1} - 1}{2} M_0^2\right)} - 1\right]$$

which, for $M_0 \leq 1$ can be approximated by

$$\gamma_{0,2} \approx \gamma_{1,2} - \left[(\gamma_{0,1} - \gamma_0)\frac{M_0^2}{M_2^2}\right] \tag{B2}$$

For sonic flow in the first nozzle ($M_2 = 1$),

$$\gamma_{0,2} \approx \gamma_{1,2} - (\gamma_{0,1} - \gamma_0) M_0^2 \tag{B3}$$

Equation (B3) has significance only for the case where the expansion through the nozzle occurs rapidly compared with the relaxation time of the gas, in which case $\gamma_{1,2} \approx \gamma_{3,4}$, and $\gamma_{0,1}$ may range from γ_0 to $\gamma_{1,2}$, depending on the stream Mach number M_0 and the probe geometry.

For hydrocarbon combustion gases where nitrogen is the main constituent, reference 11 shows the relaxation time to be

$$\tau \propto \sqrt{t}/(pW) \tag{B4a}$$

or

$$\tau = \tau_r \sqrt{\frac{t}{t_r}} \frac{p_r}{p} \frac{W_r}{W} \tag{B4b}$$

where the subscript r indicates some reference conditions. Reference 11 gives data showing $\tau = 2.3\times10^{-4}$ second for $t = 1034^\circ$ R, $p = 1$ atmosphere, and $W = 0.02$ for a nitrogen - water-vapor mixture, so that

$$\tau \approx 1.4\times10^{-7} \sqrt{t}/(pW) \tag{B4c}$$

where p is in atmospheres.

If the velocity changes in the compression and expansion occurring at the upstream nozzle are assumed to be linear with and to occur within distances of the order of the probe diameter D_e, the order of magnitude of gas velocity at which relaxation effects become significant is $2D_e/\tau$. For a probe diameter of 1/2 inch, this is roughly equivalent to stream Mach numbers of 0.2 and 0.4 for temperatures of 1000° and 4000° R and a pressure of 1 atmosphere for hydrocarbon combustion products. Thus, for this probe size with $M_2 = 1$, $\gamma_{1,2}$ may be taken as the room-temperature specific-heat ratio for the particular gas mixture; it is a function of the composition of the gases, which, of course, varies with the temperature attained in the combustion. The specific-heat ratio $\gamma_{0,1}$ is a function of the equilibrium specific-heat ratio γ_0, which varies with temperature and composition, and of the stream Mach number M_0.

On the basis of test results at a constant temperature with a variation in Mach number (fig. 8), the following empirical relation for $\gamma_{0,1}$ was established:

$$\gamma_{0,1} = \gamma_0 + (\gamma_{3,4} - \gamma_0) M_0^2 \tag{B5}$$

Substitution of this relation in equation (B3) yields the following evaluation for $\gamma_{0,2}$ in terms of γ_0, $\gamma_{3,4}$, and M_0:

$$\gamma_{0,2} = \gamma_{3,4} - (\gamma_{3,4} - \gamma_0) M_0^4 \tag{B6}$$

Application of equation (B6) in conjunction with equation (3) may be facilitated by use of graphs such as figures 9, 10, and 11, where γ_0 and $\gamma_{3,4}$ are given as functions of gas temperature, $\gamma_{0,2}$ as a function of γ_0 and M_0, and $\left[\frac{F_s(\gamma_{0,2})}{F_s(\gamma_{3,4})}\right]^2$ as a function of $\gamma_{0,2}$ and $\gamma_{3,4}$. Again an estimation of the temperature of the gas stream should be adequate.

APPENDIX C

COOLING REQUIREMENTS

The water-cooling requirements for the probe can be estimated from four heat-transfer-rate relations and one pressure-loss relation. Nomenclature used is illustrated in figure 12.

(1) The rate of heat transfer from the gas stream to the outer shell of the probe q_e can be obtained from a specification of probe diameter D_e, exposed length L_e, gas pressure, temperature, and velocity, and outer-shell temperature T_e. For this computation, gas temperature may be taken as T_0 and outer-shell temperature as average cooling-water temperature $T_{w,av}$. It is specified that the cooling-water temperature always be well below the boiling point, say 160° F. Then

$$q_e = \pi D_e L_e h_e (T_0 - T_{w,av}) \tag{C1}$$

where h_e may be obtained from

$$\frac{h_e D_e}{k_g} = 0.24 \, (Re_{D_e})^{0.6} \tag{C2}$$

(ref. 12, p. 222).

(2) The rate of heat transfer from the aspirated gas to the inner shell of the probe q_i can be obtained from the specification that

$$q_i = c_{p,g}(T_0 - T_3)w_g \tag{C3}$$

This rate can be related to the exposed internal length L_i, internal diameter D_i, Reynolds number Re_{D_i}, and inner-shell temperature T_i by

$$q_i = c_{p,g}(T_0 - T_3)w_g = h_i \pi D_i L_i \frac{T_0 - T_3}{\ln\left(\frac{T_0 - T_i}{T_3 - T_i}\right)} \tag{C4}$$

where h_i may be obtained from

$$\frac{h_i D_i}{k_g} = 0.02(Re_{D_i})^{0.8} \tag{C5}$$

(ref. 12, p. 170). For this computation, T_i may also be taken as equal to $T_{w,av}$.

In equations (C2) and (C5), the gas viscosity and thermal conductivity may be evaluated at any convenient fixed gas temperature such as $(T_0 + T_3)/2$, since the heat-transfer coefficient varies only as the 0.2 power of the gas temperature.

(3) The total rate of heat transfer to the water is the sum of q_e and q_i and produces a temperature rise ΔT_w.

$$q_e + q_i = w_w c_w \Delta T_w \tag{C6}$$

For an assumed inlet water temperature of 60° F and a specified maximum water temperature of 160° F,

$$\Delta T_w \approx 100^\circ \text{ F}$$

(4) The pressure difference needed to produce the required water flow rate will be computed under the arbitrary simplifying assumptions that a linear pressure drop exists in the cooling annulus, that pressure loss at the 180° reversal of flow direction at the probe tip can be neglected, and that the annulus may be considered as having a mean diameter $D_{av} = (D_e + D_i)/2$, a length $2L_i$, and a radial depth of $y = 1/2 [(D_e - D_i)/2 - 3x]$, where x is the average wall thickness of the three concentric tubes shown in figure 12. Then the applicable equation is:

$$\Delta p_w = \frac{24 \mu_w L_i}{\pi \rho_w y^3 D_{av}} w_w \tag{C7}$$

(ref. 12, p. 124).

If D_e, L_e, L_i, x, T_0, T_3, $T_{w,av}$, ΔT_w, and w_g are chosen in advance, then equations (C1) and (C3) give q_e and q_i directly for use in equations (C6), equations (C4) and (C5) yield the required D_i, equation (C6) yields the required w_w, and equation (C7) yields the approximate Δp_w.

This cooling must be accomplished within the following limitations:

(1) Water pressure available

(2) Heat-transfer rate obtainable between the water and the outer and inner probe walls

(3) Heat-transfer rate obtainable between the inner probe wall and the aspirated gas

(4) Local water-passage temperatures low enough not to allow formation of steam pockets

In the event that some of the requirements as outlined are not compatible with a probe design and application, a measured temperature T_3 may be inconsistent with the recommendation that it be at an accurately measurable temperature and above the dew point. In this event a heat exchanger can be placed upstream of station 3 to bring T_3 within a proper range.

APPENDIX D

ORDERS OF MAGNITUDE OF POSSIBLE ERRORS

Effect of Heat Transfer and Variation of Reynolds Number Using Flow Nozzles

5040

In the sample calculation given in appendix E, it is seen that neglect of the effect of heat transfer and the variation of Reynolds number between calibration with room-temperature air and application at high temperature would have resulted in an error of $-2\frac{1}{2}$ percent. In the present tests with hydrocarbon gases from 1500° to 4000° R, such potential errors were less than 4 percent and greater than 2 percent. In the sample calculation, had the Reynolds number variation only been considered, from figure 3, it can be seen that an error of +5 percent would have resulted. These conclusions, of course, assume the validity of equation (4).

Uncertainty in Effective Specific-Heat Ratio

From figure 11 it can be seen that the error in temperature measurement when a value of 1.4 is assumed for the effective specific-heat ratio $\gamma_{0,2}$ ranges from 2.6 to 7.8 percent for actual values of $\gamma_{0,2}$ from 1.35 to 1.25. The actual values of $\gamma_{0,2}$, as discussed previously, depend in a complex manner on the gas properties, composition, and velocity, and on nozzle geometry and method of total-pressure measurement.

In the present tests, the largest error due to neglect of the effect of stream velocity shown in figure 8 would be 4.4 percent, the datum obtained at $M \approx 1$, $T_0 \approx 2460°$ R. It would not be unreasonable to conclude, however, that for hydrocarbon-air combustion gas streams of total pressure of the order of 1 atmosphere and Mach number less than 0.5, negligible errors result from the assumption that $\gamma_{0,2} \approx \gamma_{3,4}$.

Uncertainties in Internal Temperature and Pressure Measurements

As shown by equation (3), errors in the measurement of T_3 are directly reflected in the calculation of T_0. Such errors are related to the temperature, pressure, and gas velocity at station 3 and to the diameter and immersion length of the thermocouple at that station. With reasonable attention to the design of the probe and the thermocouple, such errors may be shown to be negligible (refs. 10 and 13).

Errors in the measurements of pressures P_0 and P_3 may be considered negligible, and if pumping facilities are adequate to produce sonic flow in both nozzles for high-temperature operation, it is not necessary to measure p_2 and p_4. However, in calibration at room temperature, a probe of unity nozzle-diameter ratio will have subsonic flow in the front nozzle; therefore, static pressure p_2 must be accurately known. Hence, it is important that the static tap be properly located, free of burrs, and so forth. A 1/4-percent error in p_2 will reflect as a 1/2-percent error in T_0.

5040

Sampling Errors in Fluctuating Flow

Reference 14 shows that errors in the mean temperature measurement for a rectangular wave-form fluctuating temperature may be calculated from

$$\frac{T_{ind}}{T_{act}} = \frac{\left(1 + \frac{l_B}{l_A}\right)\left(\frac{l_B}{l_A} + \frac{T_B}{T_A}\right)}{\left(\sqrt{\frac{T_B}{T_A}} + \frac{l_B}{l_A}\right)^2}$$

where T_{ind} and T_{act} are the indicated and actual temperatures, and l_A and l_B are the fractional periods at which the gas is at temperatures T_A and T_B.

An example is given: For $T_B/T_A = 4$ and $l_B/l_A = 2$, T_{ind} would be 12.5 percent higher than T_{act}. Although this example is an extreme case, it is apparent that such errors in fluctuating flow measurements may be considerably higher than errors arising from the various other causes.

APPENDIX E

SAMPLE CALCULATION FOR EXPERIMENTAL PROBE

Probe Calibration at Room Temperature

For probe calibration at room temperature the following measured quantities and nozzle pressure ratios are specified:

P_1, P_0, p_0, in. Hg abs	29.12
p_2, in. Hg abs	21.02
P_3, in. Hg abs	24.40
p_4, in. Hg abs	12.23
T_0, T_3, $^\circ R$	540
p_2/P_0	0.722
p_4/P_3	0.501

Hence, flow is subsonic in the upstream nozzle and sonic in the downstream nozzle. Using equation (3a) with $F_1 = 0.442$ and $F_3 = 0.484$ gives

$$\left(\frac{A_2}{A_4}\right)^2 = \left(\frac{P_3F_3}{P_0F_1}\right)^2_{T_0=T_3} = 0.842$$

where

$$\left(\frac{C_2}{C_4}\right)^2_{T_0=T_3} = 1$$

since $Re_2 = Re_4$

Calculation of T_0 for High-Temperature Operation with Sonic Flow in Both Nozzles

In the calculation of T_0 for high-temperature operation with sonic flow in both nozzles the following primary measured quantities are given:

P_0, in. Hg abs	34.93
P_3, in. Hg abs	16.23
T_3, $^\circ R$	642

The secondary measured quantities are

p_0, in. Hg abs	20.33
T_w, $t_{2,n}$, $t_{4,n}$, $^\circ R$	≈ 520

Substitution of the given values into equation (3c) yields:

$$T_0 \approx \text{constant} \times T_3 \left(\frac{P_0}{P_3}\right)^2 \approx (0.842)(642)\left(\frac{34.93}{16.23}\right)^2 \approx 2500^\circ \text{ R}$$

Correction for variation in discharge coefficient with Reynolds number and heat transfer. - From figure 2, $Re_{D_{th,2}} \approx 7.6\times10^3$ and $Re_{D_{th,4}} = 1.8\times10^4$. From figure 9, $\gamma_0 = 1.286$ and $\gamma_{3,4} \approx 1.374$. The gas- to nozzle-temperature ratio is

$$\frac{t_2}{t_{2,n}} \approx \frac{T_0}{1 + \left(\frac{\gamma_0 - 1}{2} M_2^2\right)} \frac{1}{t_{2,n}} \approx 4.2$$

$$\frac{t_4}{t_{4,n}} \approx \frac{T_3}{1 + \left(\frac{\gamma_{3,4} - 1}{2} M_4^2\right)} \frac{1}{t_{4,n}} \approx 1.0$$

From figure 3, $C_2 \approx 0.966$ and $C_4 \approx 0.955$. Therefore,
$\left(\frac{C_2}{C_4}\right)^2_{hot} = \left(\frac{0.966}{0.955}\right)^2 \approx 1.022$.

Correction for effective specific-heat ratio $\gamma_{0,2}$. - Free-stream pressure ratio is $p_0/P_0 = \frac{20.33}{34.93} = 0.582$. Therefore, $M_0 \approx 0.95$. From figure 10, $\gamma_{0,2} = 1.300$; from figure 9, $\gamma_{3,4} = 1.374$; from figure 11, $\left[\frac{F_s(\gamma_{0,2})}{F_s(\gamma_{3,4})}\right]^2 = 0.961$.

Corrected T_0 (eq. (3b)). -

$$T_0 = \left[\left(\frac{A_2}{A_4}\right)^2 T_3 \left(\frac{P_0}{P_3}\right)^2\right]\left(\frac{C_2}{C_4}\right)^2 \left[\frac{F_s(\gamma_{0,2})}{F_s(\gamma_{3,4})}\right]^2$$

$$T_0 = (2500)(1.022)(0.961) = 2460^\circ \text{ R}$$

REFERENCES

1. Freeze, Paul D.: Bibliography on the Measurement of Gas Temperatures. Circular 513, Nat. Bur. Standards, Aug. 20, 1951.

2. Scadron, Marvin D.: Analysis of a Pneumatic Probe for Measuring Exhaust-Gas Temperatures with Some Preliminary Experimental Results. NACA RM E52A11, 1952.

3. Baker, Dwight I.: Mixture Ratio and Temperature Surveys of Ammonia-Oxygen, Rocket Motor Combustion Chambers. Jet Prop., vol. 25, no. 5, May 1955, pp. 217-226.

4. Simmons, Frederick S.: Analytic Determination of Discharge Coefficients of Flow Nozzles. NACA TN 3447, 1955.

5. Spooner, Robert B.: Effect of Heat-Capacity Lag on a Variety of Turbine-Nozzle Flow Processes. NACA TN 2193, 1950.

6. Grace, H. P., and Lapple, C. E.: Discharge Coefficients of Small-Diameter Orifices and Flow Nozzles. Trans. A.S.M.E., vol. 73, no. 5, July 1951, pp. 639-647.

7. Glawe, George E., and Shepard, Charles E.: Some Effects of Exposure to Exhaust-Gas Streams on Emittance and Thermoelectric Power of Bare-Wire Platinum Rhodium - Platinum Thermocouples. NACA TN 3253, 1954.

8. Glawe, George E., Simmons, Frederick S., and Stickney, Truman M.: Radiation and Recovery Corrections and Time Constants of Several Chromel-Alumel Thermocouple Probes in High-Temperature, High-Velocity Gas Streams. NACA TN 3766, 1956.

9. Buchele, Donald: A Self-Balancing Line-Reversal Pyrometer. NACA TN 3656, 1956.

10. Scadron, Marvin D., and Warshawsky, Isidore: Experimental Determination of Time Constants and Nusselt Numbers for Bare-Wire Thermocouples in High-Velocity Air Streams and Analytic Approximation of Conduction and Radiation Errors. NACA TN 2599, 1952.

11. Kantrowitz, Arthur, and Huber, Paul W.: Heat-Capacity Lag in Turbine-Working Fluids. NACA WR L-21, 1944. (Supersedes NACA RB L4E29.)

12. McAdams, William H.: Heat Transmission. Second ed., McGraw-Hill Book Co., Inc., 1942.

13. Scadron, Marvin D., Warshawsky, Isidore, and Gettelman, Clarence C.: Thermocouples for Jet-Engine Gas Temperature Measurement. Proc. Inst. Soc. Am., Paper No. 52-12-3, vol. 7, 1952, pp. 142-148.

14. Blackshear, P. L., Jr.: NACA Sonic-Flow-Orifice Temperature Probe in High-Gas-Temperature Measurement. Trans. A.S.M.E., vol. 75, no. 1, Jan. 1953, pp. 51-58.

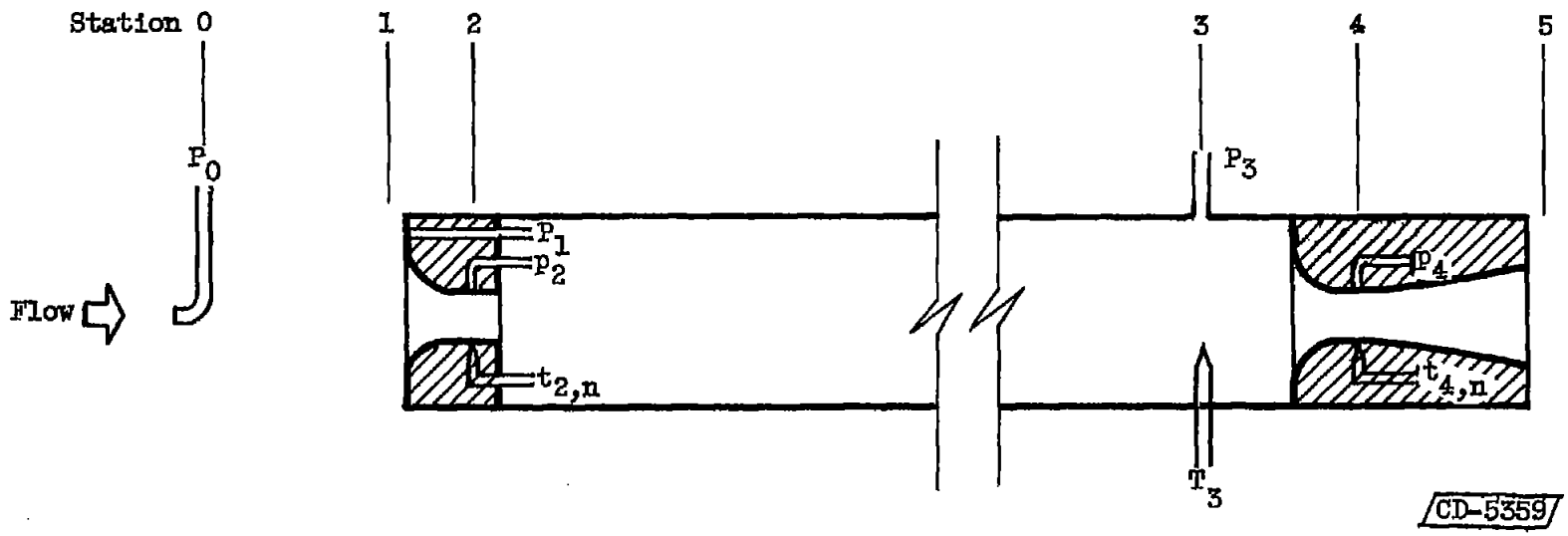

Figure 1. - Schematic diagram of pneumatic probe.

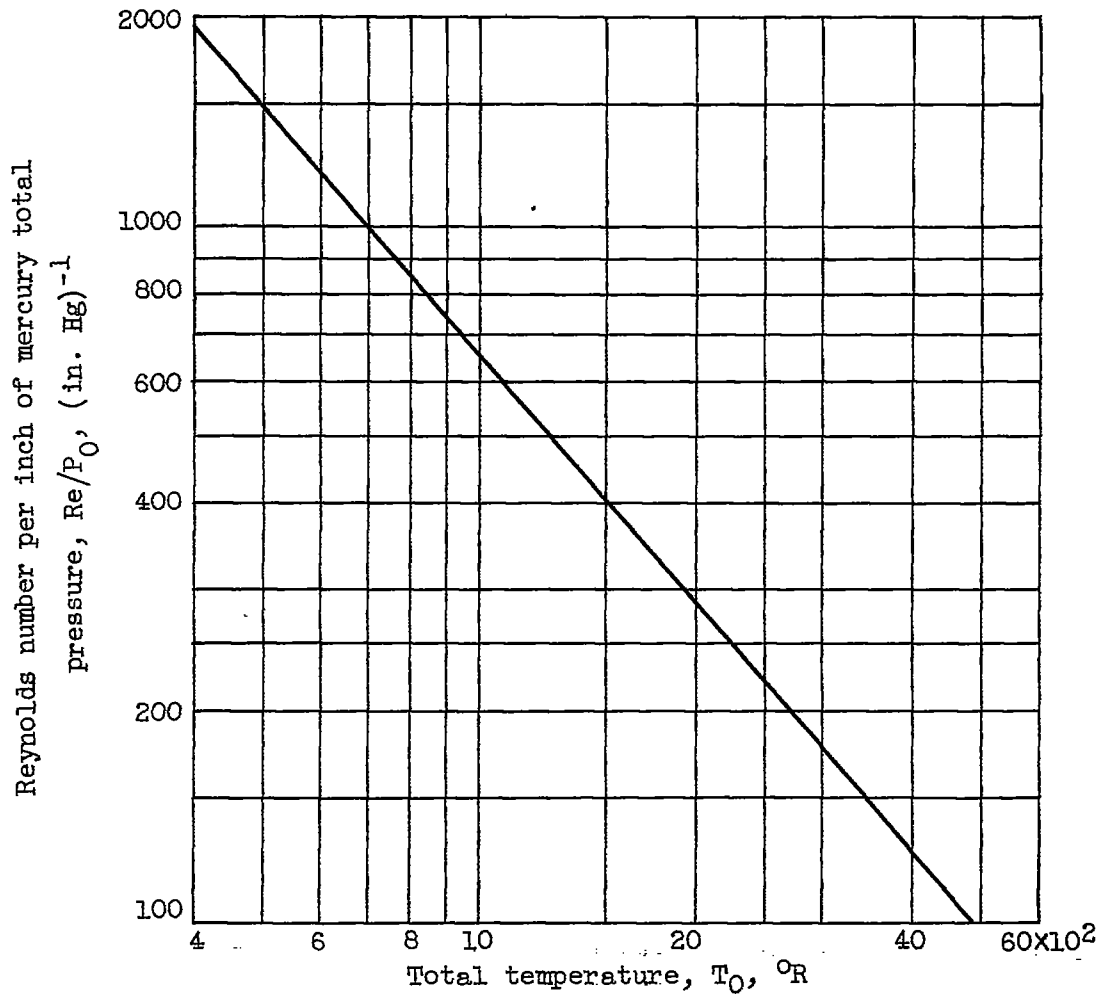

Figure 2. - Reynolds number per inch of mercury total pressure as function of total temperature for critical flow in 1/8-inch-diameter nozzle. Viscosity evaluated at total temperature; ratio of specific heats γ, 1.35.

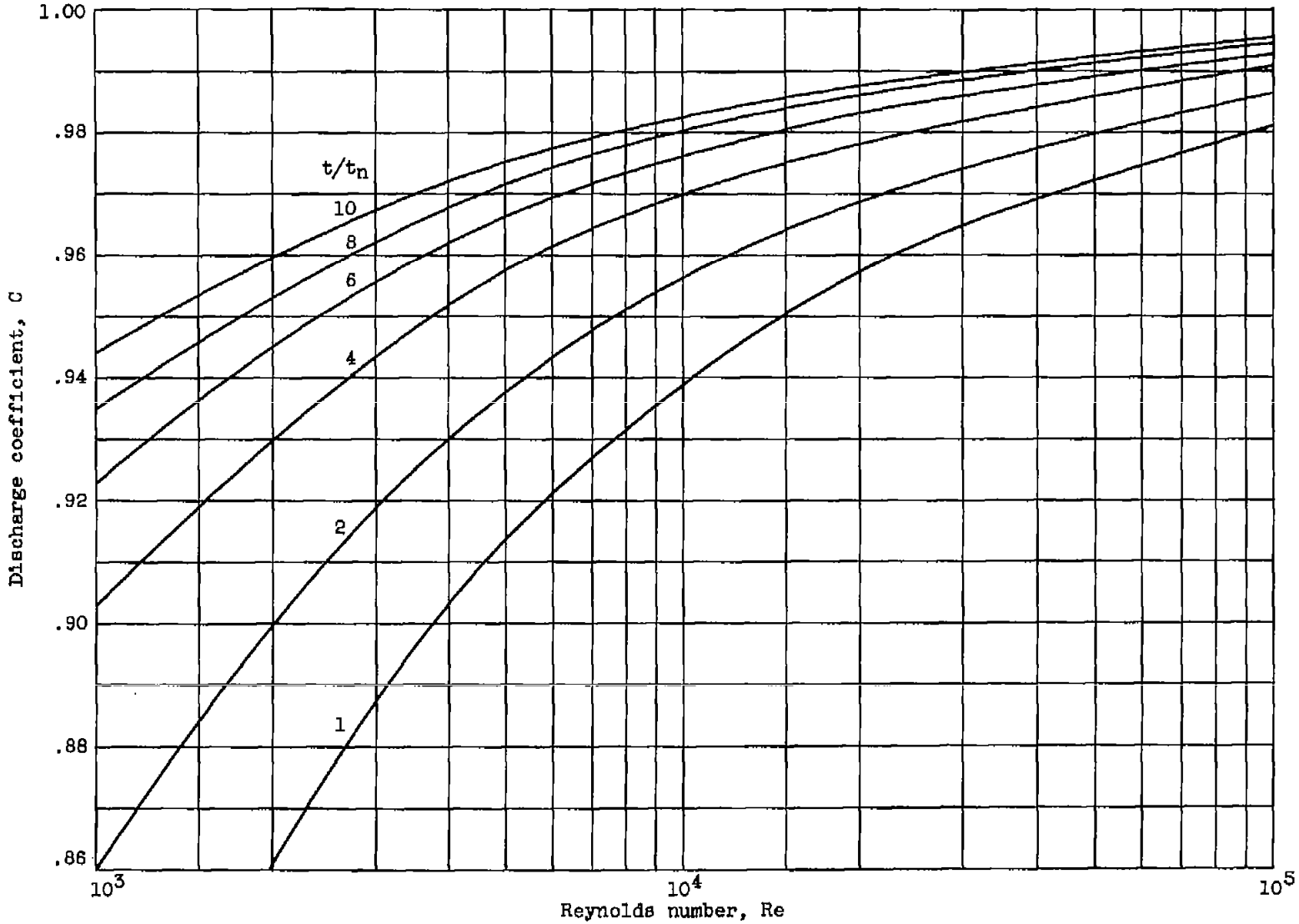

Figure 3. - Discharge coefficient as function of Reynolds number and temperature ratio. $\frac{l}{D} + \frac{1}{4}\frac{l'}{D} = 0.75$.

Figure 4. - Experimental pneumatic probe.

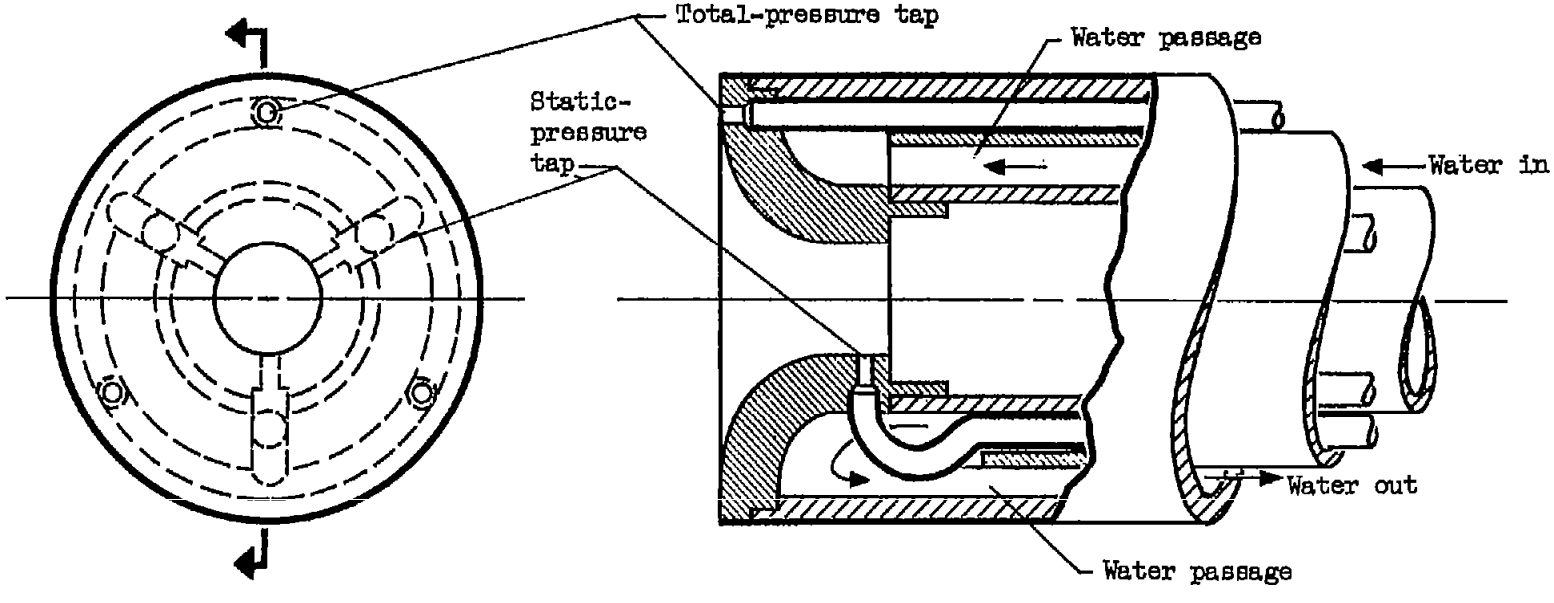

CD-5360

Figure 5. - Details of first-nozzle assembly.

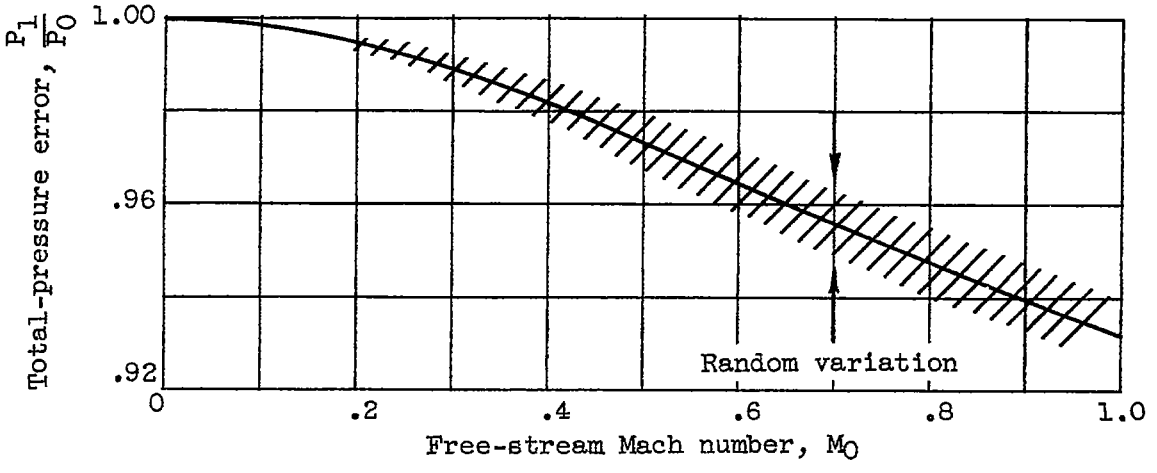

Figure 6. - Ratio of stream total pressure to indicated total pressure. Data obtained at pressures from 25 to 35 inches of mercury absolute and temperatures from 2400° to 3900° R.

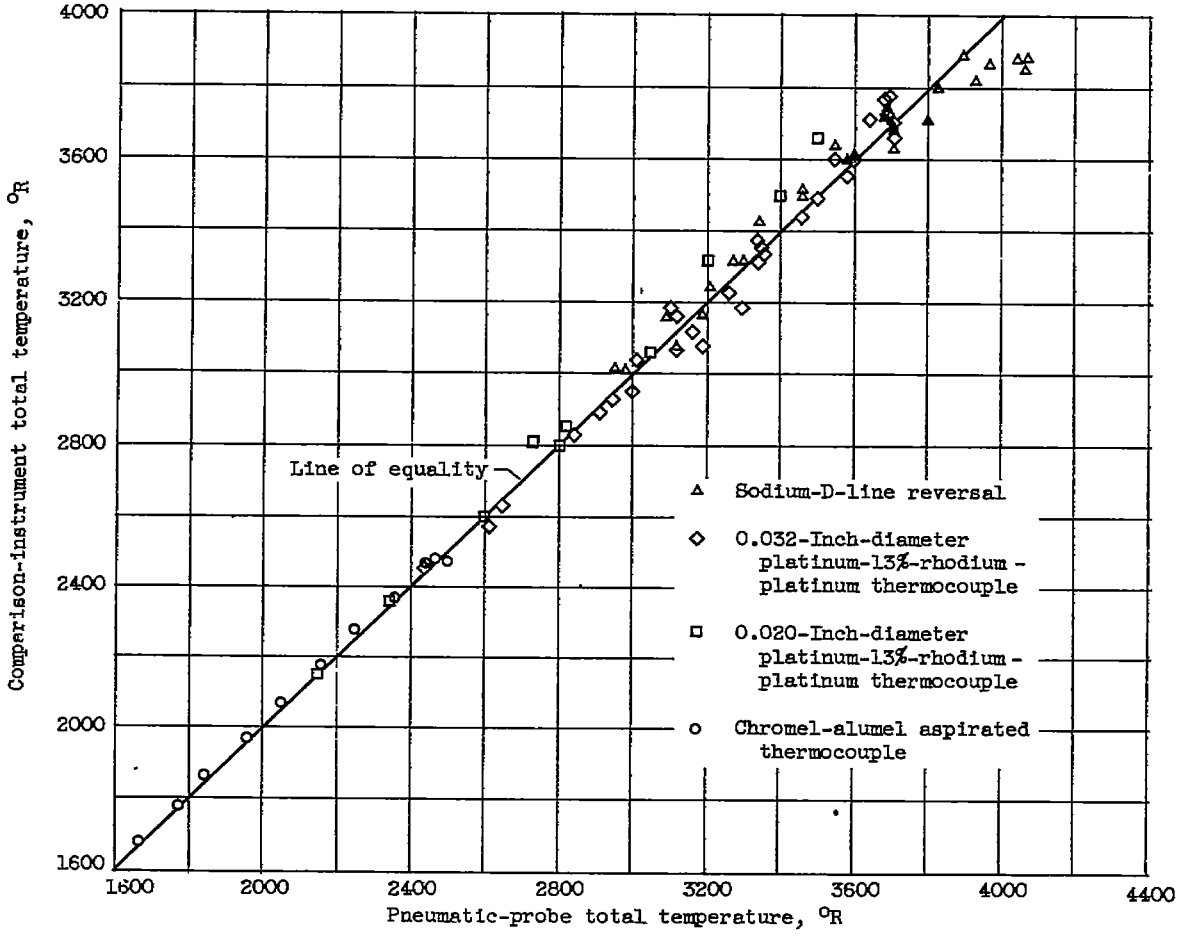

(a) With consideration of heat-transfer effect on discharge coefficient.

Figure 7. - Comparison of pneumatic-probe total temperatures with corrected indications of other instruments.

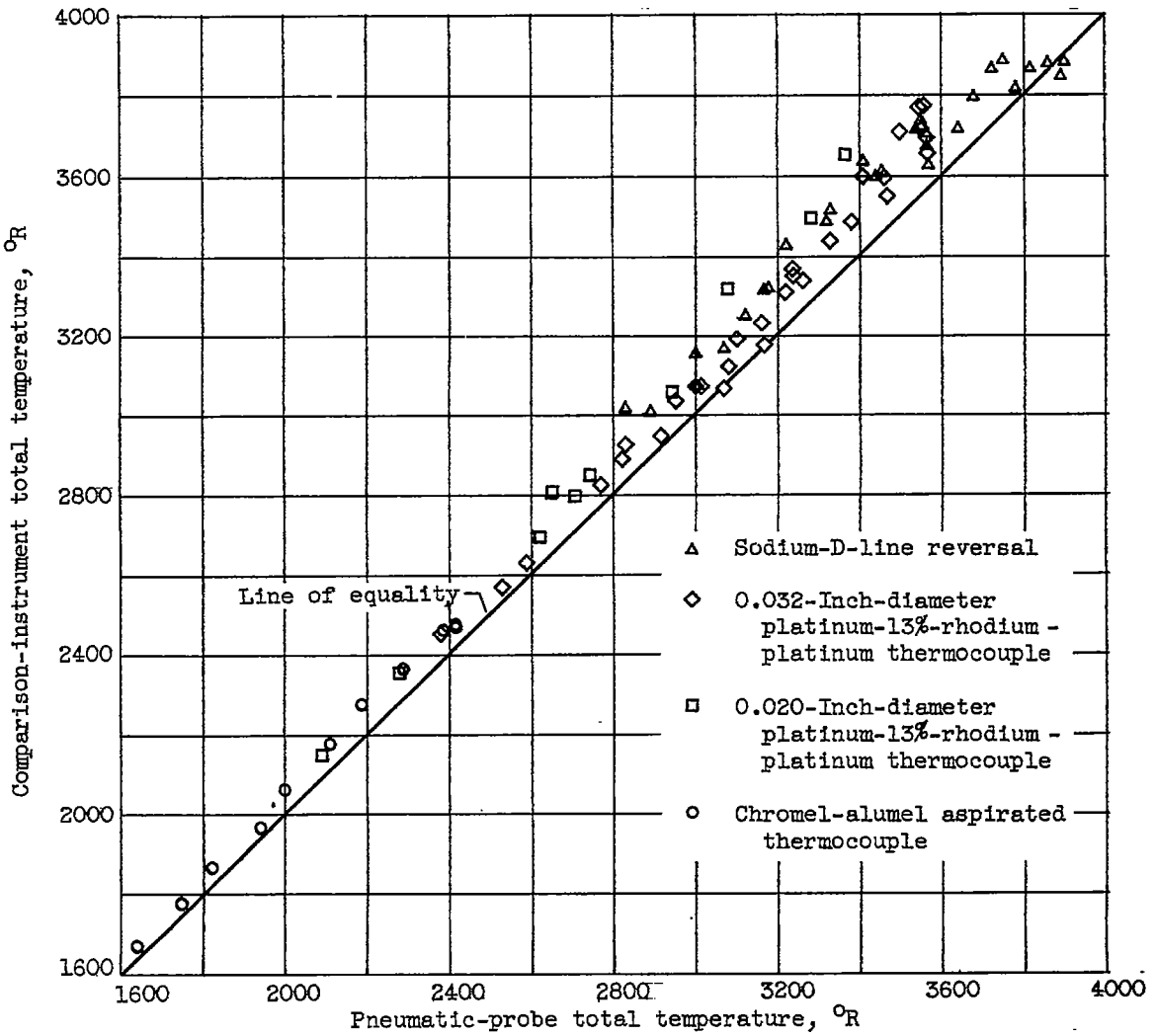

(b) Neglecting heat-transfer and Reynolds number effects on discharge coefficient.

Figure 7. - Concluded. Comparison of pneumatic-probe total temperatures with corrected indications of other instruments.

5040

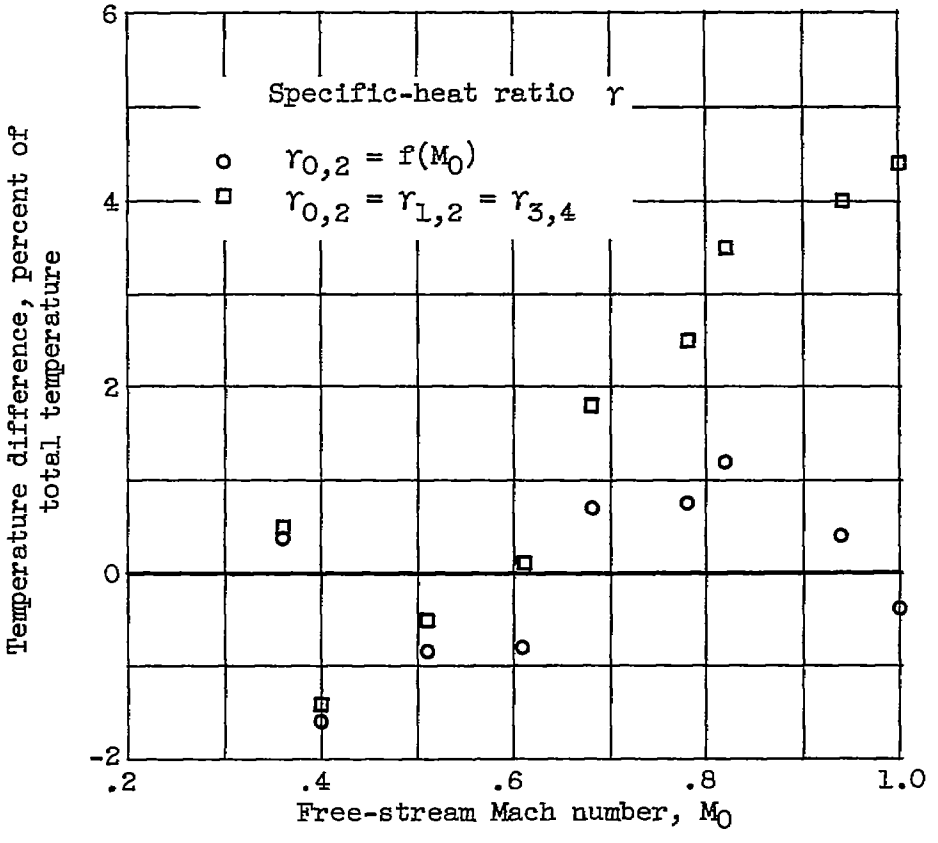

Figure 8. - Difference between calculated pneumatic-probe temperatures and aspirated-thermocouple temperatures as function of stream Mach number. Gas temperature, 2460° R.

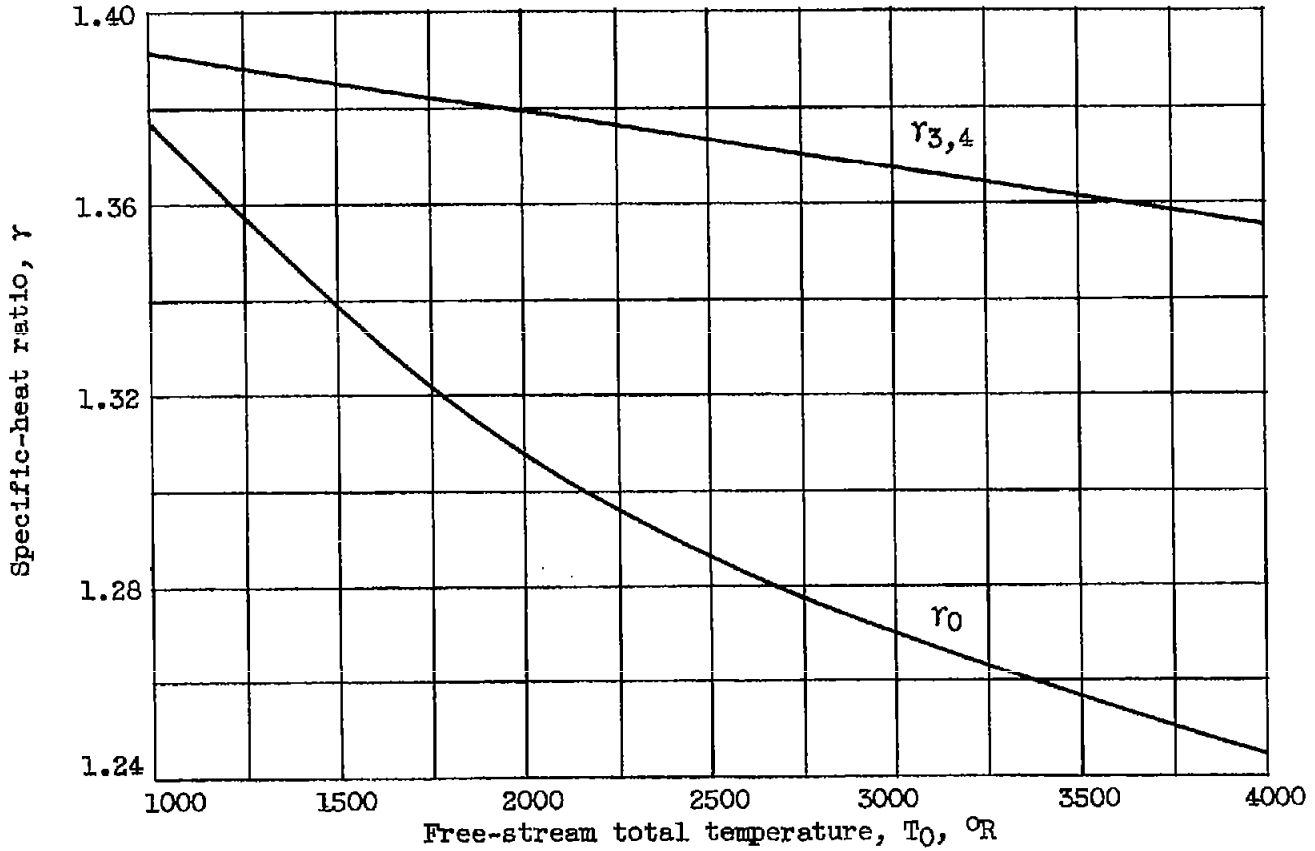

Figure 9. - Equilibrium and corresponding low-temperature specific-heat ratios for high-temperature water-cooled tunnel. Low-temperature specific-heat ratios calculated at 700° R.

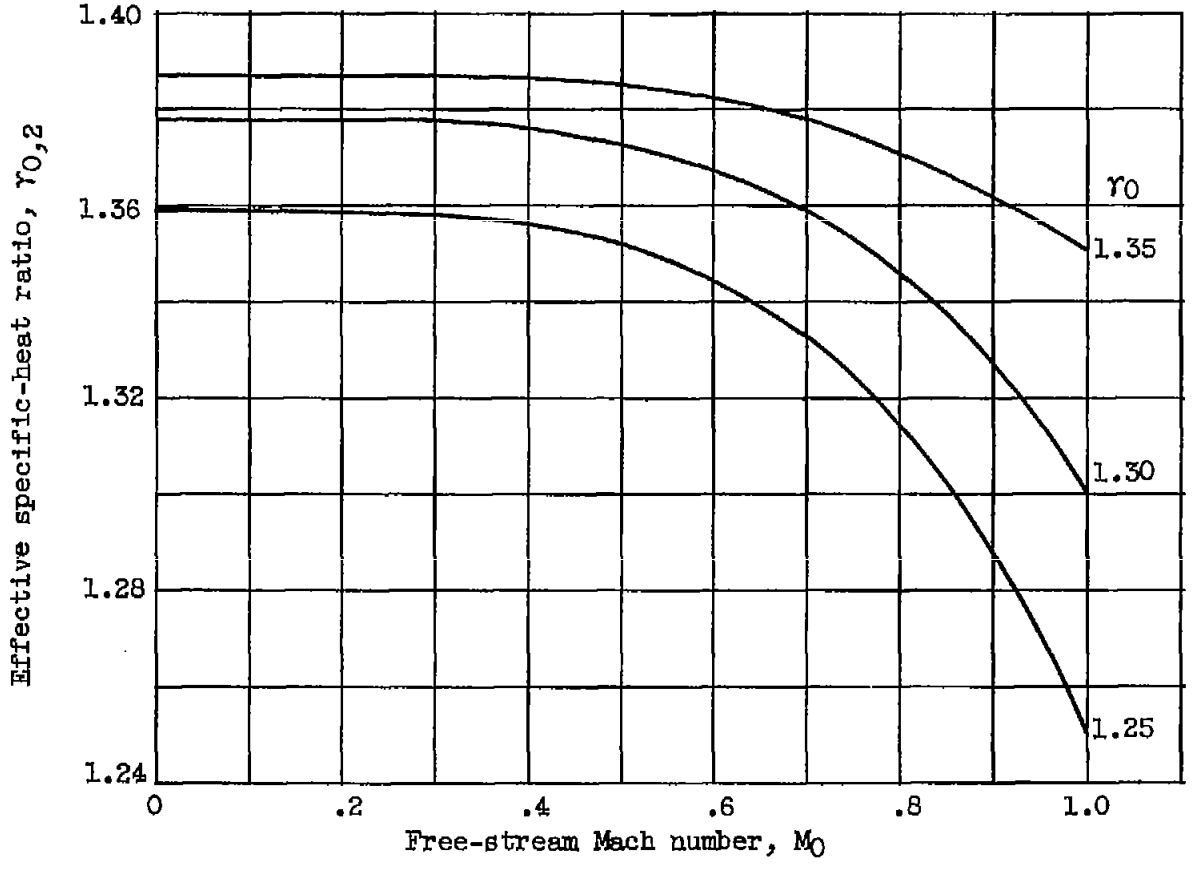

Figure 10. - Effective specific-heat ratio as function of equilibrium specific-heat ratio and stream Mach number.

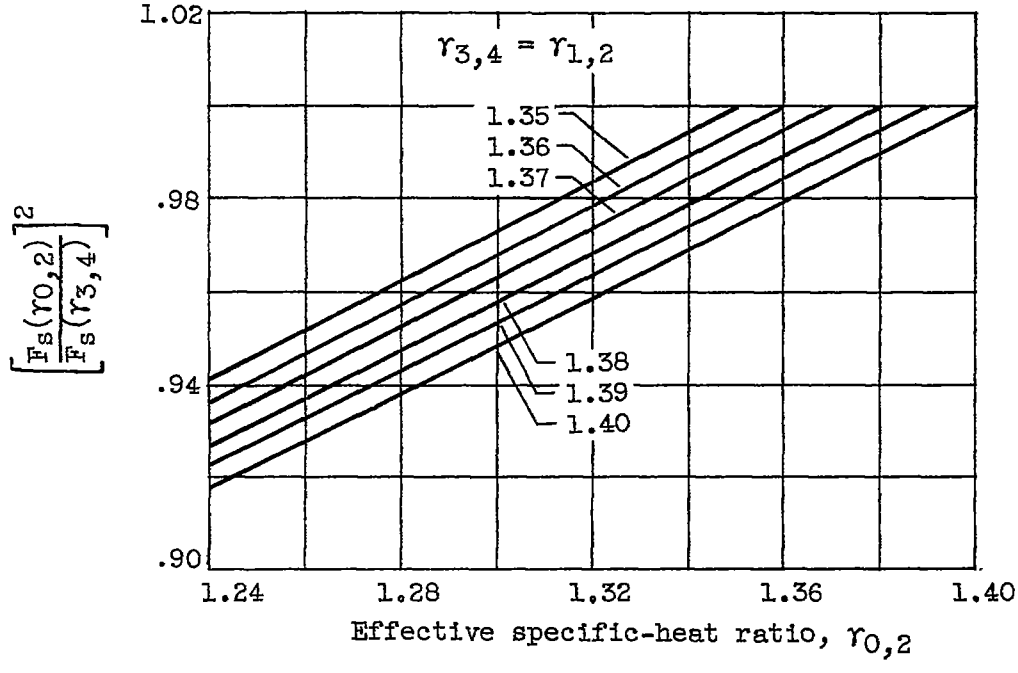

Figure 11. - Variation of function $\left[\frac{F_s(\gamma_{0,2})}{F_s(\gamma_{3,4})}\right]^2$ with $\gamma_{0,2}$ and $\gamma_{3,4}$.

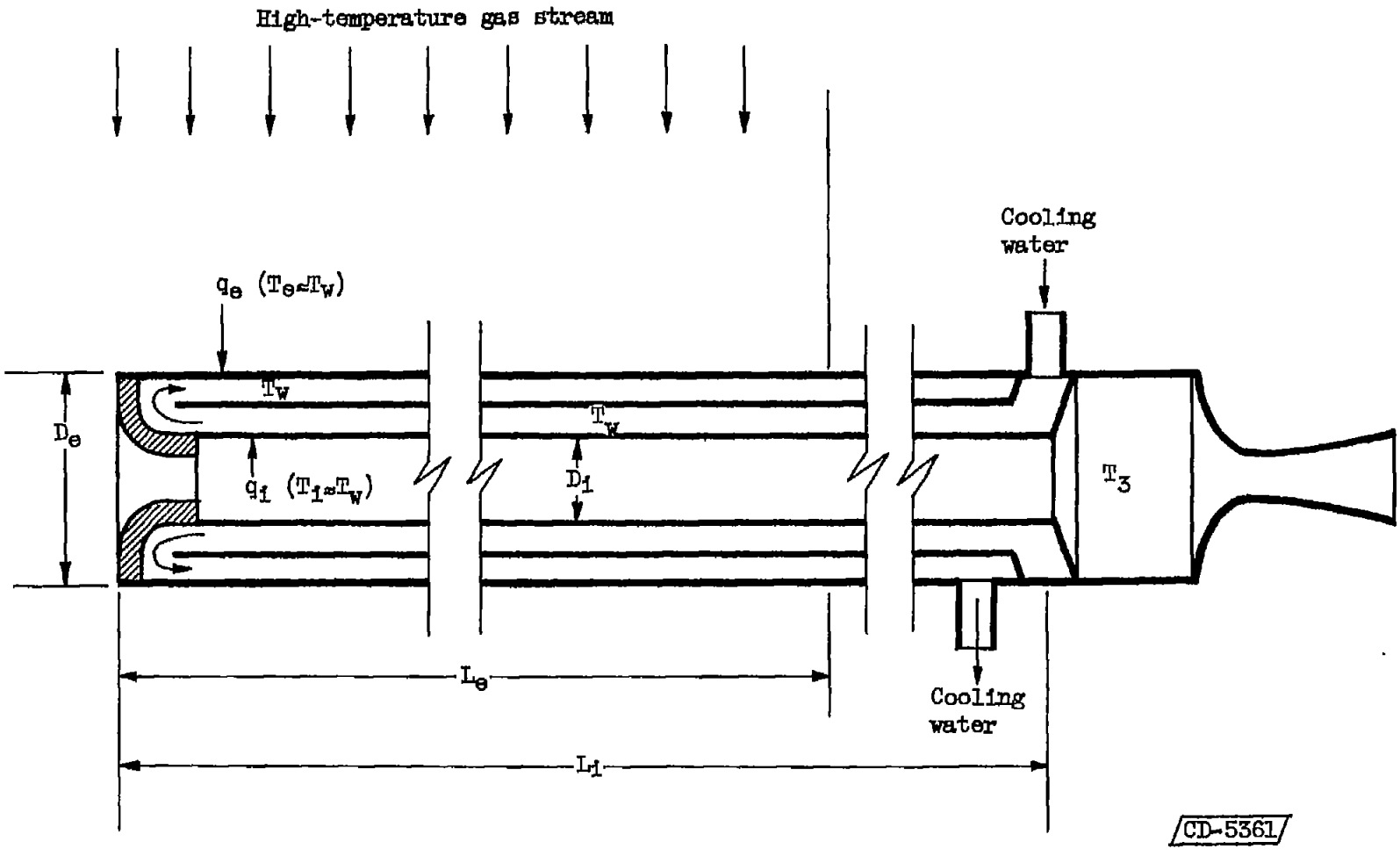

Figure 12. - Schematic diagram for cooling calculations.